Structural and electronic properties of cubic boron nitride doped with zinc

Cite as: J. Appl. Phys. **116**, 043507 (2014); https://doi.org/10.1063/1.4890607
Submitted: 14 May 2014 . Accepted: 08 July 2014 . Published Online: 24 July 2014

Yubo Li, Tianyuan Cheng, Xiao Wang, Huaxing Jiang, Hangsheng Yang, and Kenji Nose

Structural and electronic properties of cubic boron nitride doped with zinc

Yubo Li,[1,2] Tianyuan Cheng,[1] Xiao Wang,[1] Huaxing Jiang,[1] Hangsheng Yang,[3,a)] and Kenji Nose[4]

[1]*Institute of Microelectronics and Optoelectronics, Department of Information Science and Electronic Engineering, Zhejiang University, Hangzhou 310027, China*
[2]*Department of Biomedical Engineering, University of Michigan, Ann Arbor, Michigan 48109, USA*
[3]*State Key Laboratory of Silicon Materials, Department of Materials Science and Engineering, Zhejiang University, Hangzhou 310027, China*
[4]*Institute of Industrial Science, The University of Tokyo, Meguro, Tokyo 153-8505, Japan*

(Received 14 May 2014; accepted 8 July 2014; published online 24 July 2014)

Structural and electronic properties of Zn-doped cubic boron nitride (cBN) were investigated via first principle calculation based on density functional theory. Our simulation suggests that Zn can substitute for both B (Zn_B) and N (Zn_N) atom; Zn_B is energetically favorable, and Zn_N can only be prepared under B-rich conditions. Zn_B induced a shallow acceptor level; however, the large difference in electronegativity between Zn and N makes the acceptor level strongly localized, which reduces effective carrier density. In the case of Zn_N, both deep acceptor levels within band gap and shallow acceptor levels at the top of valence band were induced, which produced more free carriers than Zn_B. The calculated results account for experimental results of enhanced electric conductivity of Zn-doped cBN films prepared under B-rich conditions. © *2014 AIP Publishing LLC*. [http://dx.doi.org/10.1063/1.4890607]

I. INTRODUCTION

Cubic boron nitride (cBN), with the widest band gap of 6.3 eV among III-group Nitride semiconductors, has been extensively studied.[1] The large interest originates from its promising potential for short-wavelength light emitting diodes, semiconductor lasers, and optical detectors, as well as for high temperature, high power, and high frequency devices.[2–4] It is now possible to produce thick and stable cBN films,[5–9] however, controllable n- and p-type dopings of cBN films, necessary for high performance cBN based electronic devices, are still difficult.[10,11] From literature, S and Si were reported to be donors for cBN,[12–15] and Be, Mg, and Zn were reported as acceptors.[16–19] In fact, most of the p-type doping approaches were focused on Be impurities in cBN. Be impurities can act as a good acceptor for its shallow activation energy,[16] but the small radius of Be atom (0.44 Å) might lead to interstitial incorporation of Be, resulting in much less effective acceptor impurities.[16] Recently, the electric conductivity of Zn-doped cBN films was reported to be increased up to 10^{-2} S/cm by controlling the impurity concentration.[18] This indicated that Zn is also an excellent candidate of p-type dopants. Nevertheless, the electronic properties of Zn-doped cBN film strongly depend on the deposition conditions, and the doping process and mechanisms of carrier generation deserve further study.

In this study, we investigated the structural and electronic properties of Zn-doped cBN theoretically by using first-principle calculations based on density functional theory (DFT). Our simulation indicated that Zn can substitute for both B atom and N atom, both forming p-type conductivity of cBN, and Zn substitution for B atom is energetically favorable in thermal equilibrium. However, Zn substitution for N atom, i.e., anti-site doping, which can provide sufficient free holes, can only be prepared under B-rich deposition conditions.

II. COMPUTATIONAL DETAILS

The first principle calculations were performed using density functional theory as implemented in the CASTEP code.[20] A plane-wave basis set expanded to an energy cutoff of 310 eV and ultrasoft pseudopotential depicting the interaction between valance electrons were adopted. The exchange-correlation interaction was approximated by using local density approximation (LDA) functional in the CA-PZ scheme.[21] The integration over Brillouin zone in reciprocal space was performed using a $2 \times 2 \times 2$ Monkhorst-Pack grid for geometry optimization and then the DOS/band structure calculations. A $3 \times 2 \times 2$ supercell consisting of 96 atoms was employed and the doping process is simulated by replacing one B (Zn_B) or N (Zn_N) atom with a Zn atom, which is corresponding to the situations of Zn substitution at B and N site, respectively. It yields an effective doping level of 1.04%. The convergence was tested by using larger supercell size and higher cutoff energies, and the overall results remained unchanged. The valance electron configurations for B, N, and Zn atoms were chosen as $2s^2 2p^1$, $2s^2 2p^3$, and $3d^{10} 4s^2$, respectively. All atomic coordinates were fully relaxed, and the crystal structure optimization was performed until the energy change of per atom was less than 1.0×10^{-5} eV, the Hellmann-Feynman forces on atoms were less than 0.03 eV/Å, and the maximum displacement of per atom was 1.0×10^{-3} Å, this assures the maximum pressure of 0.05 Gpa. After full relaxation, the pressure was calculated to be less than 0.03 Gpa on a $2 \times 2 \times 3$ supercell. The electronic structures were calculated on the basis of the

a)Author to whom correspondence should be addressed. Electronic mail: hsyang@zju.edu.cn.

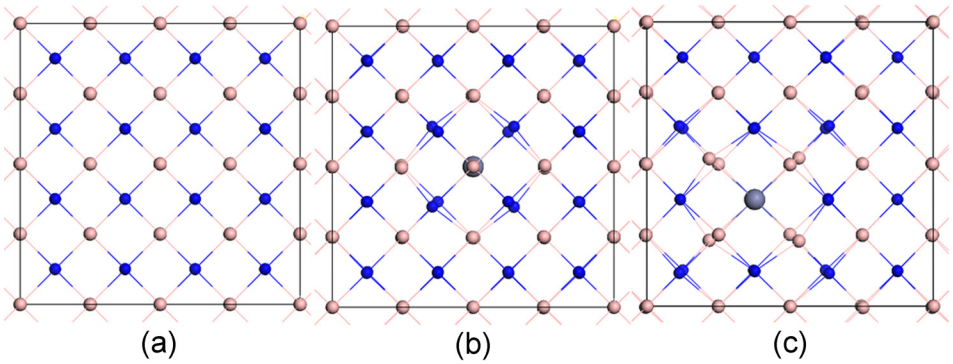

FIG. 1. Structure of ideal cBN and Zn-doped cBN with a 96-atom supercell on cBN (110) surface. (a) ideal cBN; (b) Zn substitution for B site; (c) Zn substitution for N site.

optimized supercells. For simplification, the interaction between defects is neglected, which means that all the defects are well separated.

III. EXPERIMENTAL DETAILS

The *in situ* Zn doped cBN thin films were prepared using a phase-regulated RF bias sputtering apparatus in an ultrahigh-vacuum chamber (base pressure of below 10^{-6} Pa). The experimental setup and details of deposition parameters have been described previously.[17,18] During film growth, either pure argon or a mixture of argon and nitrogen was used as plasma source gases. The Zn concentration in cBN thin films was measured by using quantitative analysis of X-ray photoelectron spectroscopy (XPS Kratos, Shimadzu) peaks of B1s, N1s, and Zn2p. Electric conductivity was measured by a van der Pauw electrode configuration using a resistivity and Hall measurement system (Resitest 8300, Toyo Corp.).

IV. RESULTS AND DISCUSSION

A. Theoretical analysis

According to structural relaxation, we found that Zn substitution causes the distortion of the spatial configuration of atoms around the inner Zn atom of the supercell. As shown in Fig. 1, using an example of a 96-atom supercell, the structure of Zn-doped cBN is quite different from that of ideal cBN on a cBN (110) surface. The bond length between Zn and its neighboring atoms (Zn_N-B, and Zn_B-N) is longer than B-N bond length of intrinsic cBN, resulting in an enlargement of lattice constant. The lattice constant of ideal cBN was calculated to be 0.3591 nm, in agreement with previous experimental measurements.[22] When cBN was doped with Zn, the lattice constant increased to be 0.3595 nm and 0.3601 nm for Zn_B and Zn_N, respectively. This is in agreement with the long bond length of Zn_N-B compared with the bond length of Zn_B-N (Table I), which also resulted in a larger local distortion of Zn_N-doped supercell. This evidence suggests that Zn substitution for N causes bigger lattice disturbance and thus needs higher formation energy (E_f). E_f of Zn doped cBN, which is dependent on the chemical potentials of the atomic constituents ($\Delta\mu$) as well as the electron chemical potential (μ_e),[23] can be written as

$$E_f = E_f' - n_e\mu_e - (\Delta n_B + \Delta n_N + \Delta n_{Zn})\Delta\mu, \quad (1)$$

where E_f' is the formation energy independent on $\Delta\mu$ and μ_e, n_e, is the number of electrons transferred from an electron reservoir, and n_N, n_B, and n_{Zn} are numbers of N atoms, B atoms, and Zn atoms, respectively. Experimentally, the atomic chemical potentials can be controlled by reaction parameters, for example, reaction conditions rich in B or N in the case of cBN film growth. So the chemical potential of the atomic constituents is restricted to[23]

$$\Delta H[BN] \le \Delta\mu_{B\,or\,N} \le -\Delta H[BN], \quad (2)$$

and the electron chemical potential is restricted to[23]

$$0 \le \mu_e \le E_g, \quad (3)$$

where E_g is the band gap, and ΔH is the heat formation. When Zn is incorporated in cBN, Zn can interact with N and B to form Zn_3N_2 and/or Zn_3B_2, respectively. Equilibrium with Zn_3N_2 and Zn_3B_2 implies[24]

$$3\mu_{Zn} + 2\mu_N = 3\mu_{Zn}[bulk] + 2\mu_N[N_2] + \Delta H[Zn_3N_2], \quad (4)$$

$$3\mu_{Zn} + 2\mu_B = 3\mu_{Zn}[bulk] + 2\mu_B[N_2] + DH[Zn_3B_2]. \quad (5)$$

Accordingly, the chemical potential $\Delta\mu_{Zn}$ should be restricted to

$$\Delta H[Zn_3N_2] \le 3\Delta\mu_{Zn} \le -\Delta H[Zn_3N_2], \quad (6)$$

$$\Delta H[Zn_3B_2] \le 3\Delta\mu_{Zn} \le -\Delta H[Zn_3B_2], \quad (7)$$

for Zn atom substitutes B and N atom, respectively. However, Zn_3B_2 formation is energetically not favored, thus even under B-rich deposition conditions, Zn_3N_2 formation is still preferred and $\Delta\mu_{Zn}$ could still be restricted to Eq. (6).

For simplification, in our calculations we neglected the temperature dependence of E_f, E_g, and ΔH in this study.

TABLE I. Parameter and formation energy of ideal cBN and Zn-doped cBN with a $2 \times 2 \times 9$ supercell.

Supercell	Charge states	Bond length (Å)	Total energy (eV)	E_f' (eV)
Intrinsic cBN	0	B-N: 1.56534	−50638.622	
Zn_B	0	Zn-N: 1.81687	−52282.089	−8.564
Zn_B^{-1}	−1	Zn-N:1.81635	−52270.359	3.166
Zn_B^{-2}	−2	Zn-N:1.81577	−52254.553	18.972
Zn_N	0	Zn-B: 1.85483	−52081.658	−0.731
Zn_N^{-1}	−1	Zn-B:1.84183	−52066.750	14.177
Zn_N^{-2}	−2	Zn-B:1.83672	−52051.095	29.832

These dependences may be important in obtaining the accurate formation energy.

Table I shows the influence of charge states on the formation energy of Zn_B and Zn_N. In this study, we deposited cBN films under negative substrate bias,[17,18] so only negative charged states of Zn doping are discussed. In the case of Zn substituting for the B atom, E_f' [Zn_B] was calculated to be −8.56 eV, which indicated that Zn_B formation is energetically favorable. The formation energy for −1 and −2 charged Zn_B increased to 3.17 and 18.90 eV, respectively, suggesting the difficulty of Zn_B negative charging. Similarly, in the case of Zn substituting N atom, E_f' [Zn_N] was calculated to be −0.73 eV, meaning that Zn_N formation is feasible; however, its preparation is more difficult compared to Zn_B. By the way, the formation of −1 and −2 charged Zn_N is energetically not favored from its high E_f' of 14.18 and 29.83 eV, respectively. Moreover, E_f of −1 charged Zn_B is always much higher than that of neutral Zn_B (as was shown in Fig. 2), indicating that Zn_B also mainly existed uncharged, though the formation of −1 charge Zn_B is possible from the view of formation energy, especially under N-rich deposition conditions. Fig. 2 also shows the influence of chemical potential on the E_f, under N-rich deposition conditions, E_f[Zn_N] (even > 0) is much higher than E_f[Zn_B], indicating Zn substituted for the B atom. When the deposition conditions changed from N-rich to B-rich, we can find that E_f[Zn_B] increased gradually while E_f[Zn_N] decreased accordingly, finally E_f[Zn_N] reduced to less than E_f[Zn_B], and Zn_N formation favored as the grey area shown in Fig. 2. According to the relationship between impurity concentration and formation energy,[24] the concentration ratio of [Zn_N]/[Zn_B] could be estimated to be approximately 1.16×10^4 under B-rich limited deposition conditions, which indicated that Zn mainly substituted N atoms. By the way, for cBN thin films prepared by vapor phase deposition, ultrahigh internal compressive stress was originated by ion bombardment during the film growth.[9] So the large distortion of Zn_N supercell also promotes Zn in B site instead of N site.

The electron density of Zn-doped cBN, using 32-, 48-, 96-, and 160-atom supercell models, is shown in Fig. 3. Compared to intrinsic cBN of the same size, additional electronic states at the top of valence band are formed when Zn substitutes for B site. When Zn substitutes for the N site, impurity energy levels are induced both within band gap and at the top of valence band. Taking a 160-atom supercell as an example, the origin of additional states can be determined from the partial density of states (PDOS) as shown in Figs. 3(c)–3(e). When Zn substitutes for the B site, Zn 4p orbital overlaps with its neighboring N 2p orbital, forming shallow acceptor levels at the top of valance band. While for Zn substitutes for the N site, Zn 4p orbital hybridizes with its neighboring B 2p orbital, inducing deep acceptor levels within band gap, meanwhile, Zn 4s orbital hybridizes with B 2p orbital, forming shallow acceptor levels at the top of the

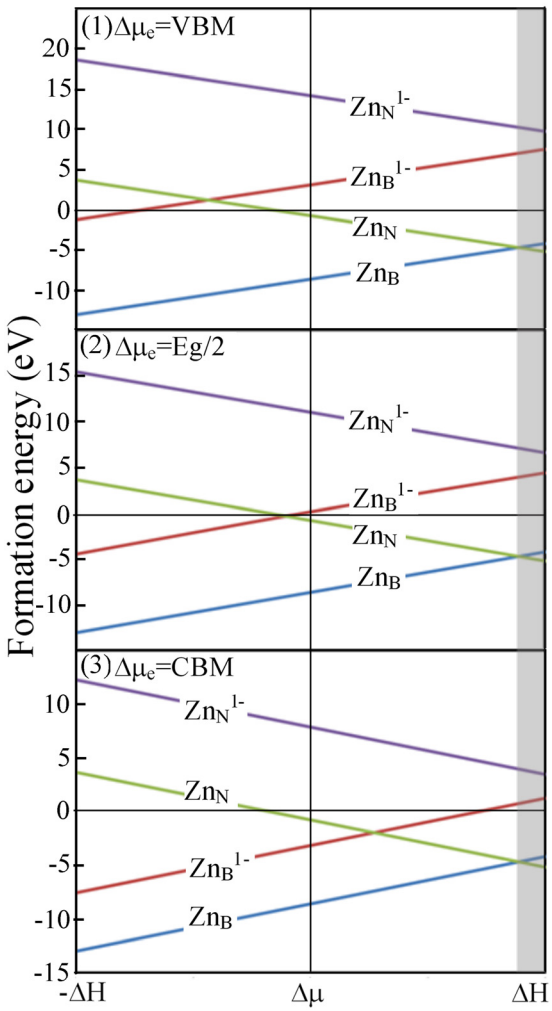

FIG. 2. Formation energies as a function of $\Delta\mu$ for three different μ_e. $\Delta\mu$ varies from the N-rich limit (−ΔH) to the B-rich limit (ΔH).

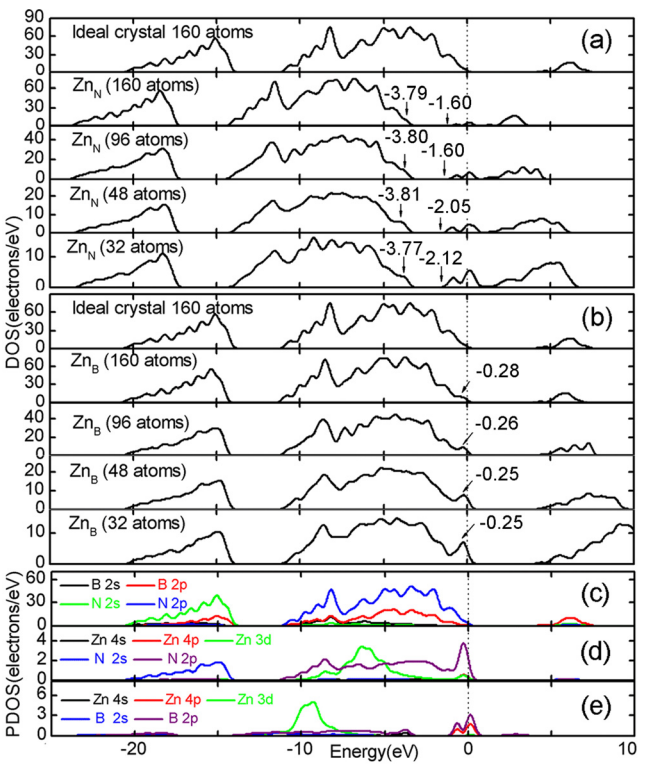

FIG. 3. Density of states of (a) Zn_N and (b) Zn_B; and partial density of states of (c) ideal cBN, (d) Zn_B with a 160-atom supercell, and (e) Zn_N with a 160-atom supercell.

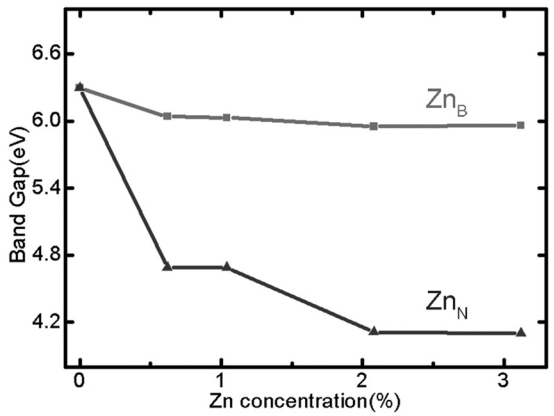

FIG. 4. Bandgap of Zn-doped cBN as a function of Zn concentration.

valance band. From the PDOS, one can also find that electrons of the Zn 3d orbital do not make bonds with other electrons, since the 3d orbital electron is the inner electron; the energy level locates in the lower position of the valence band. However, N 2p orbital electrons are repelled by Zn 3d orbital electrons, raising up the acceptor levels of Zn outer electron as shown in Fig. 3.

The calculated bandgaps of Zn-doped cBN versus Zn concentration are shown in Fig. 4, after compensation with the scissor operation of 1.9 eV,[25,26] the calculation of band structure of ideal intrinsic cBN indicates that pure cBN is indirect bandgap semiconductor material with a minimum bandgap of ~6.3 eV. The bandgap of Zn-doped cBN decreases as the Zn concentration increases. For example, the calculated bandgap decreased to 6.0 eV for Zn substitution for the B site with a doping concentration of 3.13%. Especially for Zn substitution for the N site, the calculated bandgap was as narrow as 4.1 eV with a Zn doping concentration of 3.13%. Similar phenomena were also reported in the case of S doping of cBN.[15]

In order to investigate charge distribution, the differential charge density of intrinsic cBN, together with Zn_B-doped cBN and Zn_N-doped cBN, is displayed in Fig. 5. When Zn substitutes for the B site, the electron density between Zn atom and N atom gets closer to the N atom. The same situation for Zn substituting for N site also appears, but the distortion of charge density is much weaker. This is because the electronegativity of B, N, Zn is 2.00, 3.00, 0.91, respectively, and the difference in electronegativity between Zn and N is larger than that between Zn and B.[27,28] As a result, ionicity of the Zn_B-N bond is stronger than that of Zn_N-B, and the latter's distortion of charge distribution is not as apparent as the former's. Electrons are less localized in the situation of Zn_N compared with that of Zn_B, thus offering more free carriers.

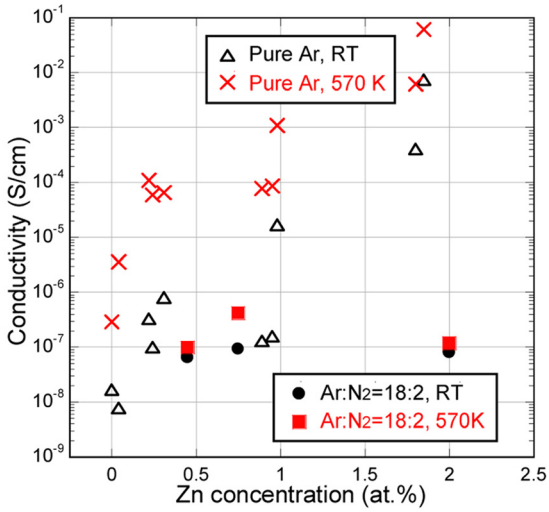

FIG. 6. Conductivity of Zn doping cBN films at room temperature and at 570 K plotted as a function of Zn concentration. Films were deposited in pure argon and a mixture of argon and nitrogen ($Ar:N_2 = 18:2$).

B. Experimental results

Figure 6 shows the conductivities of Zn-doped cBN films deposited in pure argon and 90% Ar + 10% N_2 mixture gas, respectively. According to our previous results, in the case of cBN films deposited in pure Ar, the Zn concentration in cBN is increased with B/(B + N), suggesting Zn atoms were mainly located in the N sites, namely Zn substituted for N atoms. While for films prepared in $Ar + N_2$, Zn mainly substituted B atoms.[18] From Fig. 6, the conductivities of cBN films prepared in $Ar + N_2$ were measured to be below 10^{-6} S/cm either at room temperature or at 570 K. The conductivities of cBN films prepared in pure Ar were measured to be as high as 7.4×10^{-3} and 6.1×10^{-2} S/cm at room temperature and 570 K, respectively, which are four orders of magnitude higher than those of films deposited in an Ar-N_2 mixture gas.[18]

Based on the calculated results shown in Table I and Figs. 1 and 5, we can interpret our above mentioned experimental results. It is normally expected that, in anion-rich films, impurity atom substitution for cations has lower formation energy, and substitution for anions is the opposite.[29,30] In the case of cBN with less N-vacancy, formation energy of Zn_N is too high to be realized. At the same time, interstitial doping is suppressed because of the large Zn atom

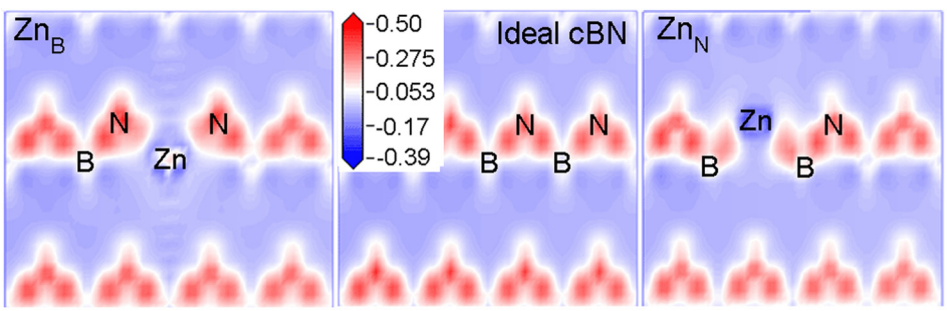

FIG. 5. Differential charge density on (110) surface of intrinsic cBN, Zn_B and Zn_N doped cBN.

size. Therefore, Zn substituted for B atom preferably occurs in ideal stoichiometry or N-rich composition, for example, cBN films deposited in $Ar + N_2$. However, the large difference in electronegativity between Zn and N induced the electrons between Zn and N to be tied around N atoms and formed big localized states, leading to difficulty in generating free carriers. As a result, the electronic doping effect is suppressed. On the other hand, in the case of films with plenty of N-vacancy, such as cBN films deposited in pure Ar (B-rich conditions), richness in B atom and N vacancy provided greater possibility to achieve Zn_N-doped cBN as the grey area shown in Fig. 2. Nonequilibrium deposition method such as sputtering, plasma enhanced chemical vapor deposition might be a key to achieve this anti-site doping in cBN thin films. As a result, free holes are generated in Zn_N-doped cBN with plenty of N-vacancies, which can result in p-type conduction in these films.[17,18] These results theoretically showed that control of stoichiometry is essential for doping in cBN film with Zn. Here, the contribution of B vacancy for the p-type conductivity was neglected, because the conductivity of cBN films prepared under similar conditions without doping is too low compared to those of the Zn doped cBN prepared in pure Ar.[31,32]

V. CONCLUSIONS

In summary, we have performed the first principle calculations to investigate the structural and electronic structure of Zn-doped cBN. Zn can substitute for both B site and N site, both forming p-type conductivity of cBN. Though Zn substitution of B atom is energetically favorable, the large difference in electronegativity between Zn and N makes the acceptor levels strongly localized, thus reducing effective carriers. Zn substitution for N atom of cBN with high p-type conductivity can only be achieved under conditions of rich in B atom and N vacancy. The theoretical approach is in accordance with experimental results of electronic conductivity of Zn-doped cBN films with different stoichiometry.

ACKNOWLEDGMENTS

This work was financially supported by the National Natural Science Foundation of China (Grant Nos. 61176051 and 50772096).

[1]N. Miyata, K. Moriki, O. Mishima, M. Fujisawa, and T. Hattori, "Optical constants of cubic boron nitride," Phys. Rev. B **40**, 12028–12029 (1989).
[2]C. H. Lin and C. W. Liu, "Metal-insulator-semiconductor photodetectors," Sensors **10**, 8797–8826 (2010).
[3]L. H. Chen, "Development of III-V semiconductor FPA photodetectors of full optical spectrum," Infrared Laser Eng. **37**, 1 (2008).
[4]A. Soltani, H. A. Barkad, M. Mattalah, B. Benbakhti, J. C. De Jaeger, Y. M. Chong, Y. S. Zou, W. J. Zhang, S. T. Lee, A. BenMoussa, B. Giordanengo, and J. F. Hochedez, "193 nm deep-ultraviolet solar-blind cubic boron nitride based photodetectors," Appl. Phys. Lett. **92**, 053501 (2008).
[5]S. Matsumoto and Z. Wenjun, "High-rate deposition of high-quality thick cubic boron nitride films by bias-assisted DC jet plasma chemical vapor deposition," Jpn. J. Appl. Phys., Part 2 **39**, L442–L444 (2000).
[6]W. J. Zhang, I. Bello, Y. Lifshitz, K. M. Chan, Y. Wu, C. Y. Chan, X. M. Meng, and S. T. Lee, "Thick and adherent cubic boron nitride films grown on diamond interlayers by fluorine-assisted chemical vapor deposition," Appl. Phys. Lett. **85**, 1344–1346 (2004).
[7]H. Boyen, P. Wedmayer, D. Schwertberger, N. Deyneka, and P. Ziemann, "Sequential ion-induced stress relaxation and growth: A way to prepare stress-relieved thick films of cubic boron nitride," Appl. Phys. Lett. **76**, 709–711 (2000).
[8]P. Ziemann, H. Boyen, N. Deyneka, P. Widmayer, and D. Schwertberger, "Periodic application of the sequence 'growth and ion-induced stress relaxation': A way to prepare stable, thick films of cubic boron nitride," Adv. Solid State Phys. **40**, 423–438 (2000).
[9]H. S. Yang, A. L. Chen, and F. M. Qiu, "Cubic boron nitride film residual compressive stress relaxation by post annealing," Diamond Relat. Mater. **20**, 1179–1182 (2011).
[10]R. H. Wentorf, "Preparation of semiconducting cubic boron nitride," J. Chem. Phys. **36**, 1990–1991 (1962).
[11]O. Mishima, K. Era, J. Tanaka, and S. Yamoka, "Ultraviolet light-emitting diode of a cubic boron nitride pn junction made at high pressure," Appl. Phys. Lett. **53**, 962–964 (1988).
[12]J. Ying, X. W. Zhang, Z. G. Yin, H. R. Tan, S. G. Zhang, and Y. M. Fan, "Electrical transport properties of the Si-doped cubic boron nitride thin films prepared by *in situ* cosputtering," J. Appl. Phys. **109**, 023716 (2011).
[13]V. A. Gubanov, E. A. Pentaleri, C. Y. Fong, and B. M. Klein, "Electronic structure of defects and impurities in III-V nitrides. II. Be, Mg, and Si in cubic boron nitride," Phys. Rev. B **56**, 13077-13086 (1997).
[14]H. S. Yang, N. Kurebayashi, and T. Yoshida, in *In Situ S-Doping of Cubic Boron Nitride Thin Films by Plasma Enhanced Chemical Vapor Deposition*, edited by T. Chandra, N. Wanderka, W. Reimers, and M. Ionescu (Trans Tech Publ, Berlin, 2010), p. 2956.
[15]Y. B. Li, H. X. Jiang, G. Z. Yuan, A. L. Chen, X. Wang, T. G. Dai, and H. S. Yang, "Electronic structure and impurity states of S-doped cBN: A first-principle study," J. Alloy Compd. **531**, 82–85 (2012).
[16]B. He, W. J. Zhang, Y. S. Zou, Y. M. Chong, Q. Ye, A. L. Ji, Y. Yang, I. Bello, S. T. Lee, and G. H. Chen, "Electrical properties of Be-implanted polycrystalline cubic boron nitride films," Appl. Phys. Lett. **92**, 102108 (2008).
[17]K. Nose, H. Oba, and T. Yoshida, "Electric conductivity of boron nitride thin films enhanced by *in situ* doping of zinc," Appl. Phys. Lett. **89**, 112124 (2006).
[18]K. Nose and T. Yoshida, "Semiconducting properties of zinc-doped cubic boron nitride thin films," J. Appl. Phys. **102**, 063711 (2007).
[19]K. Kojima, K. Nose, M. Kambara, and T. Yoshida, "Effects of magnesium doping on growth and electric conductivity of nanocrystalline cubic boron nitride thin films," J. Phys. D: Appl. Phys. **42**, 055304 (2009).
[20]S. J. Clark, M. D. Segall, C. J. Pickard, P. J. Hasnip, M. I. J. Probert, K. Refson, and M. C. Payne, "First principles methods using CASTEP," Z. Kristallogr. **220**, 567 (2005).
[21]E. M. Ann, A. S. Peter, P. D. Michael, R. M. Thomas, and L. Kevin, "Designing meaningful density functional theory calculations in materials science—A primer," Model. Simul. Mater. Sci. Eng. **13**, R1 (2005).
[22]P. B. Mirkarimi, K. F. McCarty, and D. L. Medlin, Mater. Sci. Eng. R **21**, 47–100 (1997).
[23]S. B. Zhang and J. E. Northrup, "Chemical potential dependence of defect formation in GaAs: Application to Ga self-diffusion," Phys. Rev. Lett. **67**, 2339–2342 (1991).
[24]C. G. Van de Walle and J. Neugebauer, "First-principle calculations for defects and impurities: Application to III-nitrides," J. Appl. Phys. **95**, 3851–3879 (2004).
[25]A. Janotti, D. Segev, and C. G. van de Walle, "Effects of cation d states on the structural and electronic properties of III-nitride and II-oxide wide-band-gap semiconductors," Phys. Rev. B **74**, 045202 (2006).
[26]K. Laaksonen, M. G. Ganchenkova, and R. M. Nieminen, "Vacancies in wurtzite GaN and AlN," J. Phys.: Condens. Matter **21**, 015803 (2009).
[27]J. C. Phillips, *Bonds and Bands in Semiconductors* (Academic press, New York, 1973), p. 54.
[28]K. Karch and F. Bechstedt, "*Ab initio* lattice dynamics of BN and AlN: Covalent versus ionic forces," Phys. Rev. B **56**, 7404–7415 (1997).
[29]V. A. Gubanov, Z. W. Lu, B. M. Klein, and C. Y. Fong, "Electronic structure of defects and impurities in III-V nitrides: Vacancies in cubic boron nitride," Phys. Rev. B **53**, 4377–4385 (1996).
[30]S.-H. Wei, "Overcoming the doping bottleneck in semiconductors," Comput. Mater. Sci. **30**, 337–348 (2004).
[31]K. Nose, K. Tachibana, and T. Yoshida, "Rectification properties of layered boron nitride films on silicon," Appl. Phys. Lett. **83**, 943–945 (2003).
[32]K. Nose, H. S. Yang, and T. Yoshida, "Electrical characterization of p-type cubic boron nitride/n-type silicon heterojunction diodes," Diamond Relat. Mater. **14**, 1297–1301 (2005).